Gas/Vapor Adsorption in Imogolite: A Microporous Tubular Aluminosilicate

William C. Ackerman,† Douglas M. Smith,*,† Jeffrey C. Huling,† Yong-Wah Kim,†,‡ Joseph K. Bailey,§ and C. Jeffrey Brinker†,§

UNM/NSF Center for Micro-Engineered Ceramics, University of New Mexico, Albuquerque, New Mexico 87131, Los Alamos National Laboratory, Chemical and Laser Sciences, CLS-1, Los Alamos, New Mexico 87545, and Sandia National Laboratories, Ceramic Synthesis and Inorganic Chemistry Department, Albuquerque, New Mexico 87185

Received August 14, 1992. In Final Form: January 25, 1993

Imogolite is a structurally microporous tubular aluminosilicate with one-dimensional pore channels of a single diameter that may be varied between 0.6 and 1.0 nm depending on composition. With proper processing, imogolite tubes may be synthesized and aligned into macroscopic, densely-packed arrays yielding a porous solid exhibiting a high degree of microporosity which is oriented in a single dimension as demonstrated via SEM and TEM. ^{29}Si MAS NMR indicates that with proper synthesis, essentially pure tube bundles may be obtained with very low concentrations of amorphous (nontubular) impurities as compared to purified natural imogolite. The microporous structure of natural and synthetic imogolite has been investigated by nitrogen adsorption at 77 K as a function of outgassing temperature. For synthetic samples, pore volumes are ~0.2 cm^3/g and the average pore diameter for the 100% Si sample is ~0.7 nm and is ~0.9 nm for the 50% Si/50% Ge sample. CO_2 and CH_4 adsorption at 273 K is measured over the pressure range of 0–800 Torr and uptake is influenced by tube diameter even though the surface area of the two synthetic samples is similar.

Introduction

Imogolite is a naturally occurring, hydrated aluminosilicate that derives considerable microporosity from a nanometer-sized tubular structure.[1] In contrast to several layered aluminosilicates, in which one oxygen per SiO_4 tetrahedron is shared with the gibbsite layer and the remaining three oxygen atoms are involved in SiO_4 corner-sharing, in imogolite the SiO_4 tetrahedra are isolated and effectively inverted, sharing three oxygen atoms with the gibbsite layer and leaving one oxygen as part of a silanol group. The strain associated with this increased Si–O–Al bonding is accommodated by bending the gibbsite layer, thus creating a tube having distinct external (Al–OH) and internal (Si–OH) surface characteristics (Figure 1). The composition can be written $(HO)_3Al_2O_3SiOH$, which reflects the arrangement of atoms encountered on passing from the exterior to the interior of the tube. The external tube diameter is ~2.5 nm as shown by TEM[2] and SAXS.[3] Wada and Wada[4] have shown that by substituting germanium for a portion of the silicon during tube synthesis, the tube diameter may be increased in a controlled fashion.

Most imogolite-related papers are found in the soil science and clay mineralogy literature and deal with chemical processing conditions and characterization (e.g., TEM, X-ray, solid-state NMR) of the tubular imogolite structure. While the tremendous potential of imogolite in materials science has been discussed,[5] the actual practical application of imogolite has been limited to intercalation studies in which the outer diameter of the imogolite tube is used to control the basal spacing (i.e., microporous structure) of pillared clays.[6–9] Because imogolite is also a potential molecular sieving material for membranes, catalysts, and adsorbents, our work is primarily concerned with the inner diameter and internal (SiO/OH) surface of the imogolite tubes. We are particularly interested in the one-dimensional pore network, uniform pore cross section, and narrow pore size distribution which should be possible if the tubes can be ordered to a large degree, the large pore size which fits above those

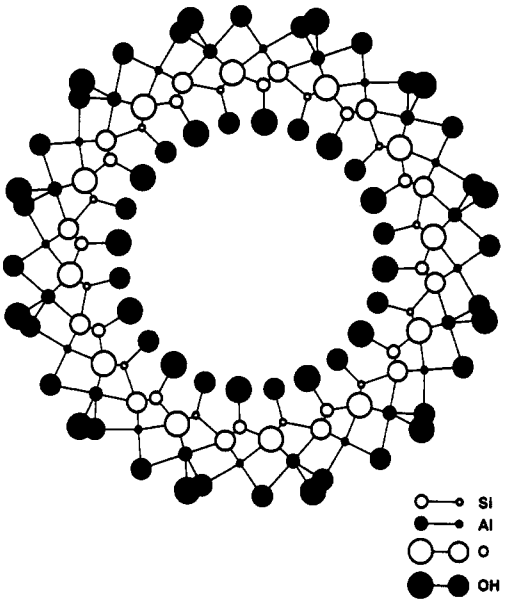

Figure 1. Structure of 100% Si imoglite.

* Author to whom correspondence should be addressed.
† University of New Mexico.
‡ Los Alamos National Laboratory.
§ Sandia National Laboratories.

(1) Cradwick, P. D. G.; Farmer, V. C.; Russell, J. D.; Masson, C. R.; Wada, K.; Yoshinaga, N. *Nature, Phys. Sci.* **1972**, *240*, 187.
(2) Kajiwara, K.; Donkai, N.; Fujiyoshi, Y.; Inagaki, H. *Makromol. Chem.* **1986**, *187*, 2895.
(3) Kajiwara, K.; Donkai, N.; Fujiyoshi, Y.; Hiraki, Y.; Urakawa, H.; Inagaki, H. *Bull. Inst. Chem. Res., Kyoto Univ.* **1985**, *63*, 320.
(4) Wada, S.; Wada, K. *Clays Clay Miner.* **1983**, *30*, 123.
(5) Farmer, V. C.; Adams, M. J.; Fraser, A. R.; Palmieri, F. *Clay Miner.* **1983**, *18*, 459.
(6) Johnson, I. D.; Werpy, T. A.; Pinnavaia, T. J. *J. Am. Chem. Soc.* **1988**, *110*, 8545.
(7) Johnson, L. M.; Pinnavaia, T. J. *Langmuir* **1990**, *6*, 307.
(8) Johnson, L. M.; Pinnavaia, T. J. *Langmuir* **1991**, *7*, 2636.
(9) Werpy, T. A.; Michot, L. J.; Pinnavaia, T. J. In *Novel Materials in Heterogeneous Catalysis*; Baker, R. T. K., Murrell, L. L., Eds.; American Chemical Society: Washington, DC 1990; pp 119–128.

0743-7463/93/2409-1051$04.00/0

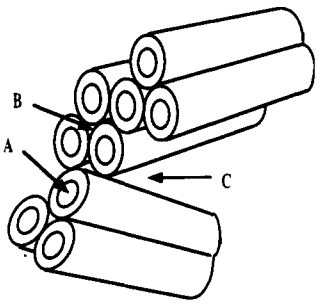

Figure 2. Conceptual diagram of the pores in imogolite.

of zeolites in the pore size spectrum,[10] and the SiOH surface which may be chemically modified to tailor pore size and surface chemistry.

Under ambient atmospheric and temperature conditions, imogolite tubes are filled with water. Since this clearly renders the tubes ineffective as gas/vapor adsorbents, it is important to know both the minimum temperature at which this water is removed and the maximum temperature that can be reached before the tube structure begins to break down. This is complicated by the fact that a number of different pore types/sizes and hydroxyl groups exist. Three different pore types are postulated for these materials as illustrated in Figure 2. These include the space within the tubes (A), the space between three aligned tubes in a regular packing (B), and mesoporosity associated with the packing of tube bundles (C). The effect of temperature on imogolite's chemical structure has been previously studied using thermogravimetric analysis, FTIR, solid-state NMR, and X-ray diffraction,[11,12] but no relation to these different pore types has been clearly shown. This is partly a result of using imogolite tubes with very little order and the fact that data interpretation is complicated by the range of defect/pore sizes associated with B and C. For example, the relationship between weight loss observed in TGA and pore emptying and dehydroxylation is unclear. With increasing temperature, one would expect the mesoporosity, C, followed by the tube pores, A, to become accessible. However, increasing temperature may cause dehydroxylation or emptying of the space between individual tubes. On the basis of an outside tube diameter of ~2.5 nm, a characteristic dimension of B is 0.3–0.4 nm. Also, the effect of SiOH or AlOH dehydroxylation on the integrity of the structure is not known.

There have been several adsorption studies using imogolite,[13–16] although none have directly measured its micropore structure. The effect of prior heating was investigated by Egashira and Aomine,[13] who found that the surface area of imogolite as measured by nitrogen adsorption at 77 K and BET analysis was maximized after heating to 300 °C. Adams[14] outgassed two imogolite samples (natural and synthetic) at 200 °C and measured the accessible micropore volume as a function of adsorbate molecular size using nitrogen at 77 K and water, several small hydrocarbons (benzene and smaller), and perfluorotributylamine at elevated temperatures (140–207 °C). Nitrogen adsorption indicated that both samples contained significant mesoporosity. For the elevated temperature adsorption measurements, a gas chromatography technique was employed. Micropore volumes as measured with water were significantly lower than with nitrogen, raising the question of whether equilibrium was obtained in the GC adsorption measurements. However, a molecule's size effect on micropore volume was observed with the microporosity being completely inaccessible to the perfluorotributylamine (kinetic diameter = 1.02 nm[10]). Wada and Henmi[15] used adsorption of various salts from solution to assess pore size and inferred pore sizes of ~1 nm in size. However, these types of measurements are not directly related to gas adsorption. Wada and Yoshinaga[16] measured the density of natural imogolite using various size liquids and found a strong effect of size which also demonstrated the microporous nature of these materials.

These past studies of pore structure and adsorption in imogolite suffer from several shortcomings including the significant degree of mesoporosity associated with the random tube packing in both natural and synthetic imogolite samples employed and uncertainty concerning the roles of heat treatment/outgassing on pore structure and adsorption properties (i.e., under what conditions is adsorbed water removed from the different pores and under what conditions does dehydroxylation of SiOH and AlOH occur).

Experimental Procedure

Farmer and Fraser[17] described a method for synthesizing imogolite in very dilute (millimolar) solutions of $Al(ClO_4)_3$ and $Si(OH)_4$. The imogolite yield was found to be maximized, relative to boehmite and other nontubular products, by maintaining low precursor concentrations, starting with an excess of $Si(OH)_4$ (Si/Al ~0.6 vs the stoichiometric ratio of 0.5), and by an initial, temporary (i.e., immediately reversed) increase in solution pH to partially neutralize the aluminum salt and promote imogolite nucleation. Significant amounts of imogolite were formed in the sol by heating at 95–100 °C for 1 day, although heating for 5 days gave the best results. The yield of synthetic imogolite was estimated by measuring the volume of gel obtained by flocculating the sol at pH ~ 10 with NH_4OH and centrifuging.

Our approach modifies that of Farmer and Fraser by "seeding" the formation of imogolite. By adding a portion of a previously processed synthetic imogolite sol to a mixture of 2.5 mM $Al(ClO_4)_3$ and 1.25 mM $Si(OH)_4$, we have found that the pH adjustment step can be avoided, excess orthosilicic acid does not increase the imogolite yield, and imogolite formation is nearly complete after heating at 95–100 °C for 2 days. The seeding sol, added in a 1:4 weight ratio to the precursor solution, is ultrasonically dispersed (10 min, 20 kHz, ~10 W) prior to addition to increase the concentration of potential imogolite growth sites. With a proper collection and drying procedure,[18] we have found that a high degree of tube ordering can be obtained and the amount of the mesoporosity minimized.

Previously, Wada and Wada[4] have shown that by replacing a fraction of the silicon precursor with a germanium precursor, that the Al–O–Ge bond angles were such that the tube diameter could be increased in a systematic fashion. Following this approach, we have produced tube bundles using a starting solution in which 50% of the silicon has been replaced with germanium and were subsequently ordered. Since not all of the germanium and silicon is necessarily incorporated into tube bundles, the actual composition of germanium and silicon in the tubes may be different than 1/1 (weight basis). Therefore, elemental analysis was conducted by fusing the powder with NaOH, leaching with water followed by HCl, and performing flame atomic absorption spectroscopy. AAS indicated that of the silicon and germanium sites, the sample is ~50.3% silicon. For comparison to the

(10) Breck, D. W. *Zeolite Molecular Sieves*; J. Wiley and Sons: New York, 1974.
(11) MacKenzie, K. J. D.; Bowden, M. E.; Brown, I. W. M.; Meinhold, R. H. *Clays Clay Miner.* **1989**, *37*, 317.
(12) van der Gaast, S. J.; Wada, K.; Wada, S. I.; Kakuto, Y. *Clays Clay Miner.* **1985**, *33*, 237.
(13) Egashira, K.; Aomine, S. *Clay Sci.* **1974**, *4*, 231.
(14) Adams, M. J. *J. Chromatogr.* **1980**, *188*, 97.
(15) Wada, K.; Henmi, T. *Clay Sci.* **1972**, *4*, 127.
(16) Wada, K.; Yoshinaga, N. *Am. Miner.* **1969**, *54*, 50.
(17) Farmer, V. C.; Fraser, A. R. In *International Clay Conference 1978*; Mortland, M. M., Farmer, V. C., Eds.; Elsevier Science Publishers: Amsterdam, 1979; pp 547–553.
(18) Huling, et al. US Patent Application, 1992.

Figure 3. SEM micrograph of 100% Si synthetic imogolite showing the long range order of the collected material.

synthetic samples, natural imogolite was provided by K. Wada, following a chemical purification treatment[19] to remove organic matter, extractable oxides, and nontubular amorphous silicates.

Nitrogen adsorption experiments were performed at 77 K using a static volumetric method (Micromeritics ASAP 2000M adsorption analyzer) over the relative pressure range $\sim 10^{-6} < P/P_0 < 0.99$. BET surface areas were determined from adsorption at five relative pressures in the range 0.05–0.20. Micropore area, micropore volume, and micropore size distribution were determined from *t*-plots interpreted using the MP method.[20] Differential pore volume plots were determined using the Horvath–Kawazoe[21] model with the Saito–Foley modification[22] to reflect the actual cylindrical rather than slit-shaped geometry (assumed in the H–K method) of the imogolite micropores. We should note that Figure 1 of ref 22 is incorrect and we have recalculated the relationship between partial pressure and pore size using the equations from that reference (which are correct). Total pore volume was estimated from nitrogen uptake at $P/P_0 \sim 0.99$. Methane and carbon dioxide adsorption was measured at 273 K over the pressure range of 0–800 Torr using a Micromeritics ASAP-2000 automated adsorption analyzer.

SEM was performed using a field emission of SEM (Hitachi S-800) after coating of the samples with platinum. TEM of the tube bundles was accomplished with a JEOL 2000-FX 200-keV TEM. ^{29}Si MAS NMR was conducted at 79.459 MHz using a Varian Unity 1 NMR. Samples were spun at ~7 kHz and delay times of 30 to 1000 s were employed. XRD was measured using a Scintag Pad-V with a step scan of 0.02° over the 2θ range of 2° to 30° for Cu Kα radiation. TGA was performed over the temperature range of 20–700 °C using a Perkin-Elmer TGA-7 with a heating rate of 10 °C/min.

Results and Discussion

The SEM micrograph in Figure 3 shows a synthetic imogolite agglomerate in which the visible "threads" are tube bundles, each containing many individual (~2.5 nm outer diameter) imogolite tubes. This layered structure is similar in appearance to the gel films of natural imogolite that form on volcanic ash due to weathering.[23] Natural imogolite agglomerates, however, typically have more open, weblike structures. In natural imogolite, the 10–30 nm width of the bundles limits the range of ordering,[19] whereas in the more dense synthetic materials, the imogolite tubes are ordered over hundreds of nanometers. This longer range of ordering for our synthetic material should result in greatly reduced mesoporosity. This can be seen in the TEM micrographs (Figure 4) which show that the tight packing of the synthetic imogolite appears to exclude all extraneous, nontubular material from the structure. Electron diffraction confirms that the repeat distance perpendicular to the lines in Figure 4a for the 100% Si material is ~2.6 nm, corresponding to the outer diameter of the imogolite tubes. Figure 4b is a similar micrograph for the 50% Si material. For this sample, the tube length does not appear to be as great as for the 100% Si sample but the tubes are still highly ordered and no amorphous material is evident. The shorter tube length for germanium-containing samples was previously observed by Wada.[4] There does not appear to be a significant difference in the tube diameter between the two samples as observed via TEM.

The fraction of an aluminosilicate sample which is tubular is difficult to determine via X-ray diffraction since the small tube size and high degree of orientation preclude accurate XRD analysis. XRD was attempted for both synthetic imogolite samples and showed a broad peak at *d*-spacing >12 Å. Although quantitative information was obtained, the 100% Si imogolite had a more intense peak located at smaller *d*-spacing than the 50% Si sample. In contrast to XRD, the ^{29}Si MAS NMR spectrum for the 100% Si sample exhibits a sharp, characteristic peak at approximately −78 ppm which is assigned to a silicon bonded through oxygen to three aluminum atoms and having a single silanol group.[23] From the integrated area under this peak, as compared to that of the broad peak characteristic of amorphous aluminosilicate gels, the fraction of silicon in an ordered environment may be estimated. Deconvolution of the spectra for the purified natural imogolite sample indicates that only ~40% of the Si is in an ordered environment. ^{29}Si MAS NMR spectra are shown in Figure 5 for both natural and synthetic samples and clearly demonstrate the highly tubular nature of the synthetic sample. ^{29}Si MAS NMR was not performed on the 50% Si sample because the lower silicon concentration and small quantities of samples which were available precluded adequate signal to noise. When the 100% Si synthetic sample was heated (ambient to 110 to 275 °C), no change in the position or shape of the −78 ppm peak was noted but the relaxation time (T_1) of the silicon atoms increased from ~30 to ~500 to ~4000 s with increasing temperature. If dehydroxylation occurred, one would expect a downfield shift of approximately 10 ppm as silicon condenses to form SiOSi bridges. The constant chemical shift implies that dehydroxylation of the Si does not occur under these conditions and the increasing relaxation times are a result of lower concentrations of water in pores A and B. Heating at 275 °C before adsorption analysis typically resulted in an additional weight loss of 0.05–0.1 g/g (as compared to 250 °C) which is consistent with the release of tightly bound of water in pores B. This weight loss is observed between 225 and

(19) Wada, K. *Am. Mineral.* **1967**, *52*, 690.
(20) Mikhail, R.; Brunauer, S.; Bodor, E. *J. Colloid Interface Sci.* **1968**, *24*, 45.
(21) Horvath, G.; Kawazoe, K. *J. Chem. Eng. Jpn.* **1983**, *16*, 470.
(22) Saito, A.; Foley, H. C. *AIChE J.* **1991**, *37*, 429.
(23) Barron, P. F.; Wilson, M. A.; Campbell, A. S.; Frost, R. L. *Nature, Phys. Sci.* **1982**, *299*, 616.

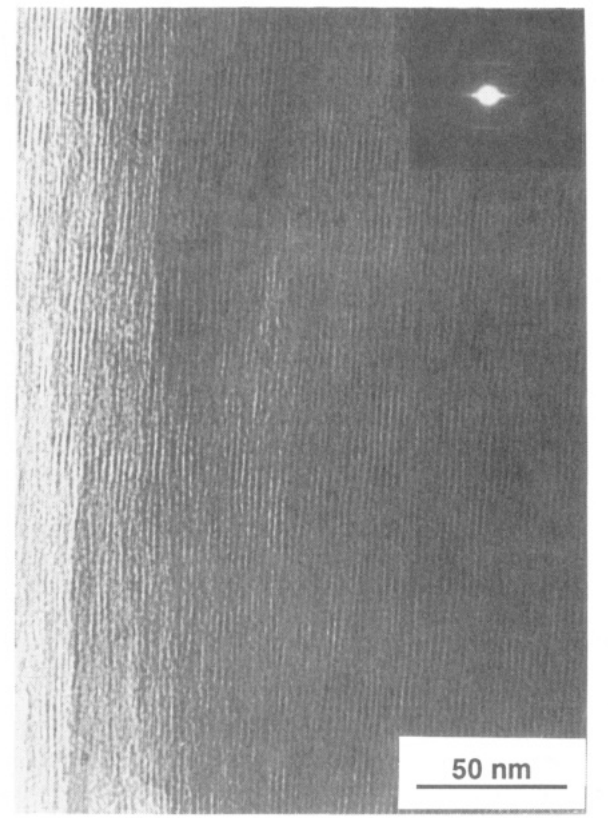

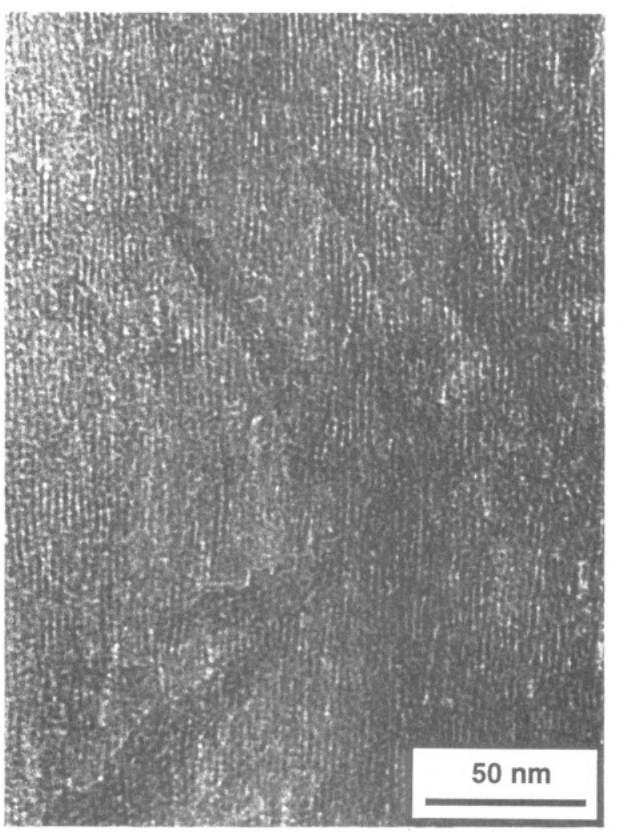

Figure 4. (a, top) TEM micrograph and electron diffraction of 100% Si synthetic imogolite showing local ordering and tube spacing of approximately 2.5 nm. (b, bottom) TEM micrograph of 50% Si synthetic imogolite showing local ordering and tube spacing of approximately 2.5 nm.

250 °C for the 50% Si sample which is consistent with a slightly larger tube size.

To more precisely determine the micropore structure of natural and synthetic imogolite, we have determined

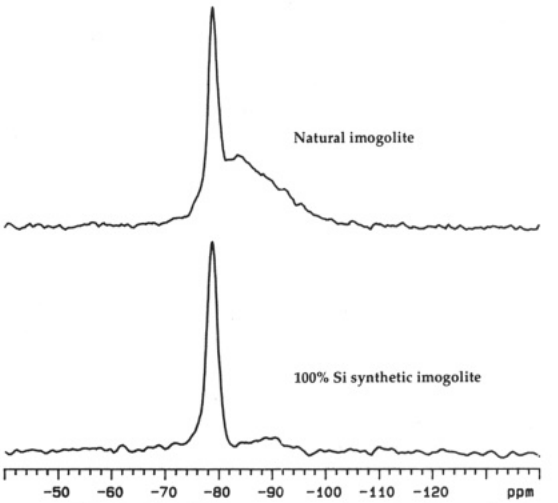

Figure 5. ^{29}Si MAS NMR spectra of 100% Si synthetic and natural imogolite (referenced to TMS).

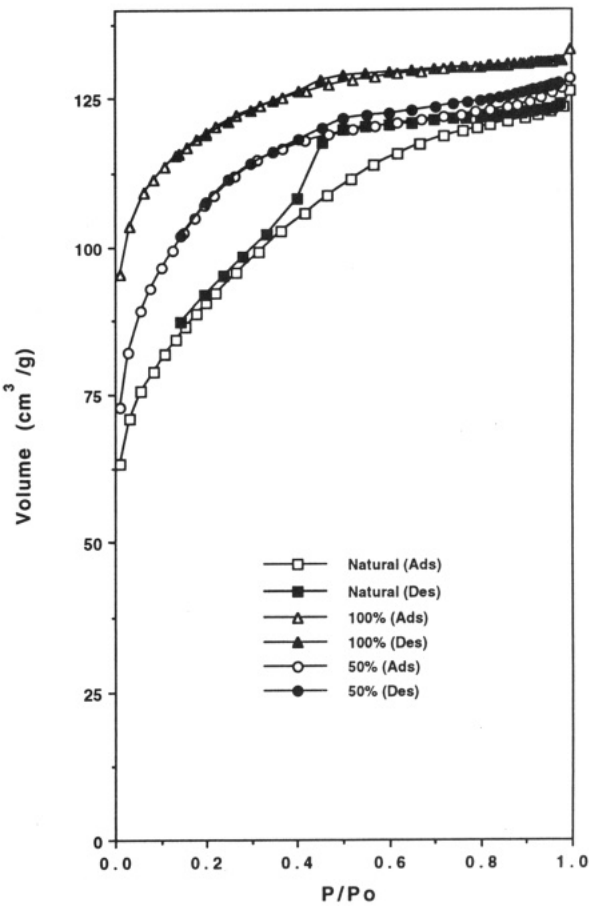

Figure 6. Nitrogen adsorption/desorption isotherms at 77 K for natural and synthetic imogolite (100% Si and 50% Si).

adsorption isotherms beginning at much lower relative pressures than in previous studies[12,13], $P/P_0 \sim 10^{-6}$, and following outgassing for ~12 h at incrementally increasing temperature under vacuum. Adsorption–desorption isotherms are given in Figures 6 (high pressure) and 7 (low pressure) for the three different imogolite samples (natural, synthetic, Si/Ge) after outgassing at 275 °C. The much greater long-range order of the synthetic imogolite samples is readily apparent from the enhanced adsorption uptake at $P/P_0 < 0.2$. This is also manifested in reduced mesoporosity for the synthetic samples as indicated by the lack of hysteresis in the desorption branch of the isotherm in the 0.3–0.99 P/P_0 range. We should note that

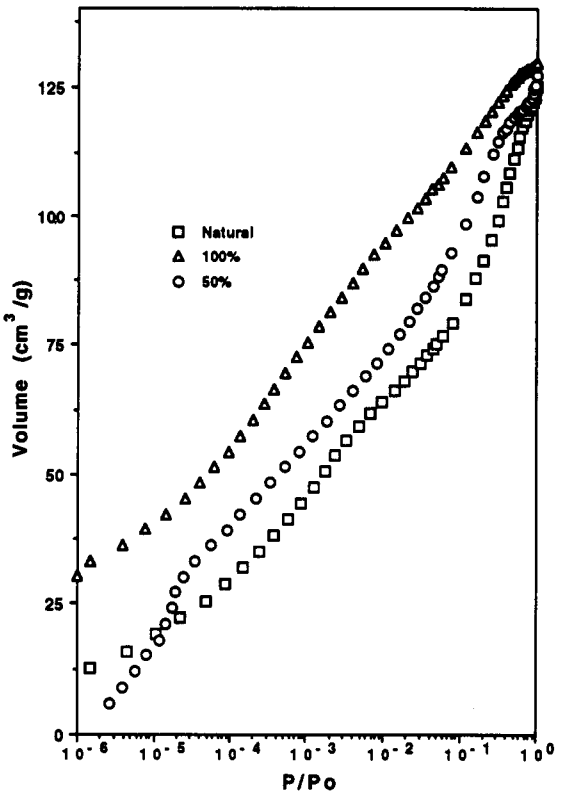

Figure 7. Low pressure nitrogen adsorption isotherms at 77 K for natural and synthetic imogolite (100% Si and 50% Si).

since the measurement of adsorption isotherms in microporous materials is somewhat dependent upon experimental conditions (outgassing, pressure transducer accuracy, equilibration times, etc.), the quantitative comparisons of these isotherms with literature isotherms for molecular sieves should be avoided but qualitative comparisons between imogolite and the molecular sieves should be valid.

As discussed previously, the change in imogolite pore structure as a function of outgassing temperature is unclear from the current literature. Figure 8 shows adsorption isotherms for the 100% Si synthetic sample as a function of outgassing temperature (225, 250, 275 °C). For the 275 °C sample, a large increase in uptake of low relative pressure ($P/P_0 < \sim 10^{-6}$) is observed. This low relative pressure uptake of ~ 30 cm^3 STP/g is consistent with the weight loss observed upon outgassing. This result is also consistent with the ^{29}Si MAS NMR results which support the desorption of water from micropores B.

From the nitrogen adsorption isotherms, we have calculated typical pore structure parameters such as BET

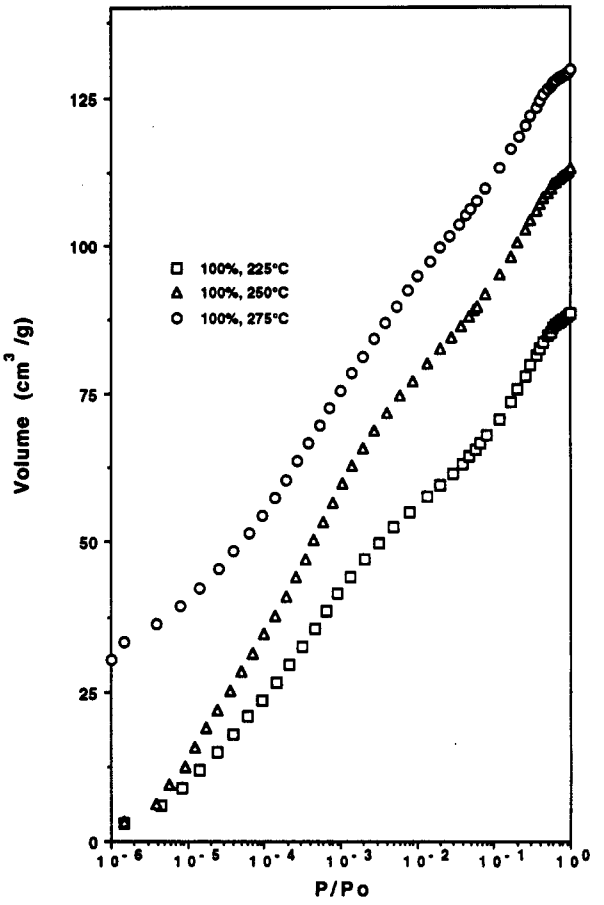

Figure 8. Effect of outgassing temperature on nitrogen adsorption isotherms for the 100% Si synthetic imogolite.

surface area, total pore volume, micropore surface area, and hydraulic radius (twice the ratio of pore volume to surface area) as a function of outgassing temperature and these are reported in Table I. We should note that caution must be applied in the application of BET analysis to microporous materials since the concept of unconstrained multilayer adsorption is of limited validity although the same general trends are observed if the adsorption data is analyzed via Langmuir analysis. As expected from Figure 6, the synthetic samples exhibit a much higher fraction of the pore volume and surface area which is microporous (pores less than 1 nm in radius). Of particular note is the ratio of micropore to total (BET) surface area which exceeds 0.8 for the synthetic samples under higher temperature outgassing conditions. The uptake of nitrogen at low relative pressures ($P/P_0 < 0.1$) presented in Figure 7 shows that there is a clear size difference between

Table I. Pore Structure Parameters as a Function of Outgassing Temperature Determined from Nitrogen Adsorption at 77 K

	200 °C	225 °C	250 °C	275 °C
natural imogolite				
A_s, BET surface area (m^2/g)	255	257	270	318
micropore area (m^2/g)	80	89	104	160
V_p, pore volume (cm^3/g)	0.167	0.167	0.171	0.193
mean pore radius, $2V_p/A_s$ (nm)	1.31	1.30	1.27	1.21
synthetic imigolite (100% Si)				
A_s, BET surface area (m^2/g)	240	259	340	398
micropore area (m^2/g)	156	177	258	324
V_p, pore volume (cm^3/g)	0.129	0.137	0.175	0.201
mean pore radius, $2V_p/A_2$ (nm)	1.07	1.06	1.03	1.01
synthetic imogolite (50% Si/50% Ge)				
BET surface area (m^2/g)		297	332	403
micropore area (m^2/g)		196	267	290
pore volume (cm^3/g)		0.157	0.175	0.211
mean pore radius, $2V_p/A_s$ (nm)		1.06	1.05	1.05

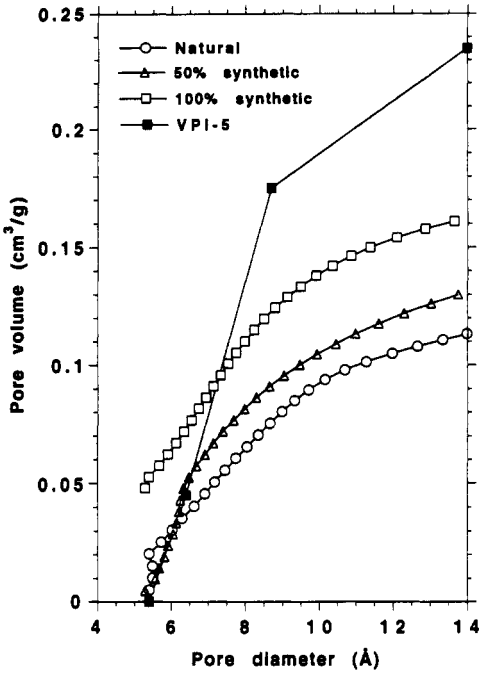

Figure 9. Cumulative modified HK pore size distributions for imogolite out-gassed at 275 °C and VPI-5.[24]

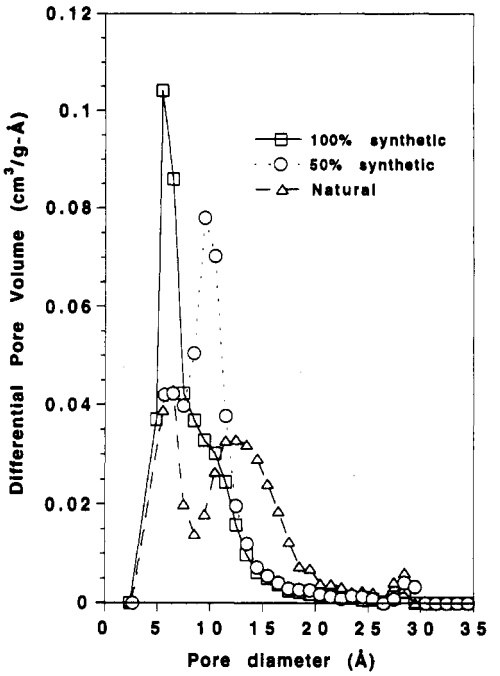

Figure 10. Differential pore size distributions using the MP method for imogolites outgassed at 275 °C.

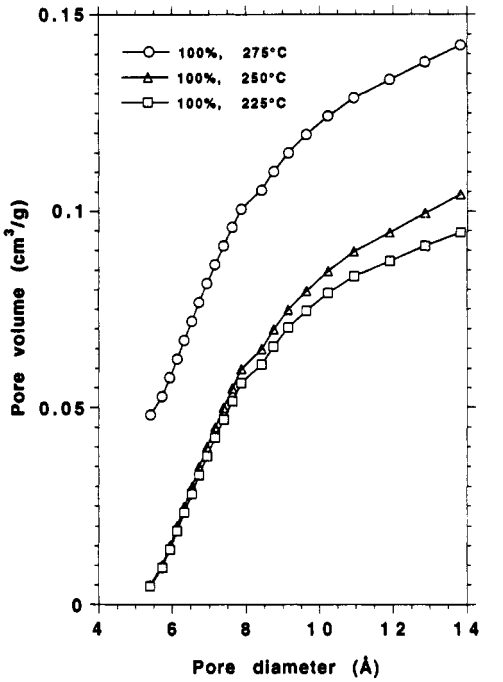

Figure 11. Effect of outgassing temperature on modified HK cumulative pore size distributions for the 100% Si synthetic imogolite.

the synthetic samples which is 100% Si and the sample containing 50% Ge replacement for Si. The nitrogen uptake in the natural imogolite sample, which has similar pore size to that of synthetic 100% Si sample, varies significantly as a result of nontubular, amorphous impurities. For all samples, both the pore volume and surface area increase with increasing outgassing temperature as smaller pores are emptied of water. This is consistent with increasing micropore surface area and a decrease in the mean (hydraulic) pore radius.

From the low pressure adsorption data in Figure 7, the size distribution of the micropores can be estimated using the Saito–Foley cylindrical pore modification of the HK method[22] (or any of several other methods) and these are shown in Figure 9. Cumulative pore size distributions are reasonably narrow and the pore diameter (via modified HK) is in the range of 0.5–1.5 nm. These sizes are in agreement with those estimated from electron and X-ray diffraction and postulated from the imogolite structure.[1] The sample containing 50% germanium and 50% silicon in the silicon sites exhibits a slightly larger pore size than the 100% silicon sample but still has a narrow distribution indicating that the germanium is distributed in the tubes. For qualitative comparison, we have calculated the pore size distribution for VPI-5, a molecular sieve with pore dimension of ~1 nm, obtained by applying the modified HK method to the argon adsorption data reported by Davis and co-workers.[24]

Many methods may be used to relate adsorption relative pressure to size in the micropore size region; however, these methods are much more sensitive to model assumptions, adsorbate properties, and adsorbent properties than analysis of adsorption/condensation for mesopore size analysis. Therefore, instead of employing only the modified HK method, we have also analyzed the adsorption data of Figure 8 with the MP/t-plot method.[20] Differential pore size distributions for the three imogolite samples outgassed at 275 °C are shown in Figure 10. The 100% Si synthetic imogolite exhibits a fairly narrow distribution centered at a pore diameter of ~0.7 nm as compared to the ~0.9 nm diameter of the 50% Si sample. The 50% Si sample also has a small peak at ~2.8 nm which is a result of the small amount of mesoporosity in this sample. The natural imogolite has a much larger peak at ~2.8 nm which results from a much larger fraction of mesoporosity as compared to the synthetic samples. The natural imogolite also exhibits a bidisperse size distribution in the micropore region. A sharp peak is observed at ~0.7 nm corresponding to the tubular structure and a broad peak between 1.2 and 2.5 nm corresponds to the amorphous gel material. For all three samples, the resolution of the MP method is insufficient to observe the difference in pore size between A and B.

(24) Davis, M. E.; Saldarriaga, C.; Montes, C.; Garces, J.; Crowder, C. *Zeolites* **1988**, *8*, 362.

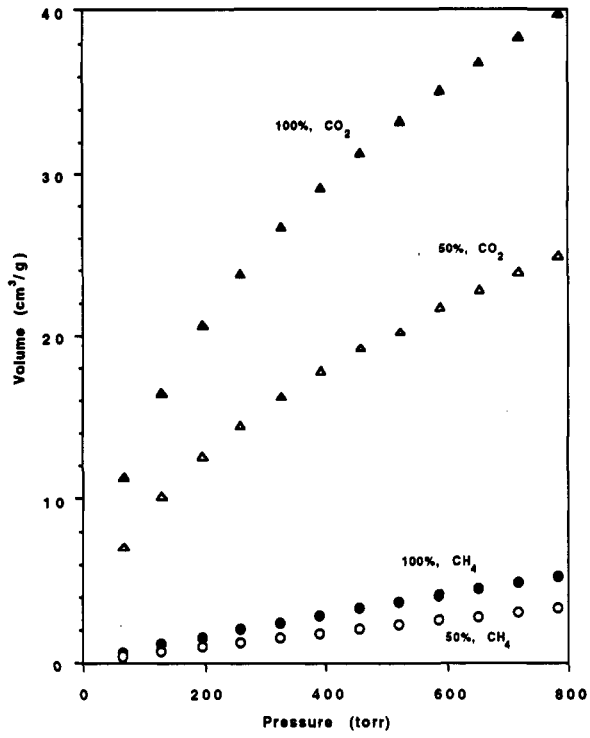

Figure 12. Methane and carbon dioxide adsorption isotherms at 273 K for synthetic imogolite (100% and 50% Si).

On the basis of the structure of imogolite (Figures 1 and 2) and the SEM/TEM observations (Figures 3 and 4), one might expect that the cumulative pore size distributions for the synthetic imogolite samples shown in Figures 9 and 10 might be more monodisperse. However, we interpret this as a combination of two factors. These adsorption measurements were made over approximately 12 h and equilibrium might not yet have been obtained in these microporous materials and the fact that the modified HK and MP methods may not describe adsorption in these materials precisely. In the application of the Saito–Foley modification of the HK method to zeolite Y, monodisperse pore size distributions were also not observed.[22]

During outgassing, changes in the modified HK pore size distribution are observed as additional water is removed from the tubes (A) at lower temperature and from the inner tube pores (B) at higher temperatures. The effect of this on the cumulative micropore size distribution with the pore diameter calculated using the modified HK method is shown in Figure 11 for the 100% Si synthetic sample. The pore size distribution for pores with diameter greater than ~0.6 nm is essentially constant for these three temperatures. However, outgassing at 275 °C offsets the cumulative pore volume by the volume of the small pores, B. Pore sizes cannot be directly assigned to B since pore filling occurs at relative pressures less than the resolution limit of our instrument (10^{-6}).

In addition to low temperature (77 K) adsorption of nitrogen, we have also measured adsorption of methane and carbon dioxide from 0 to 800 Torr at 273 K (see Figure 12). It is interesting to note that methane and carbon dioxide uptake at a given pressure is significantly higher for the 100% Si sample as compared to the 50% sample even though the total specific surface area of the two samples is essentially identical (see Table I). For both methane and carbon dioxide adsorption at 800 Torr, the 100% Si sample adsorbs ~1.6 times that of the 50% Si sample. Since both the surface chemistry (SiOH and SiOH/GeOH) and surface area of these samples are very similar, the enhanced uptake for the 100% sample is presumably a result of the higher adsorption potential resulting from the slightly smaller tube diameter.

Conclusions

By synthesizing imogolite using a seeding step followed by a colloidal ordering process prior to drying, essentially phase-pure tubular imogolite is obtained which is highly ordered and exhibits essentially no amorphous gel or associated mesoporosity. The pore structure of the synthetic imogolite consists of ~0.2 cm^3/g of micropores with two distinct pore types formed by the inner tube volume and the interstitial space between three tubes packed in a hexagonal array. The characteristic diameter of these two pore types is <0.4 and ~0.7 nm. Whereas the large pores are opened to adsorbing gas after removal of condensed water at 200 °C under vacuum, the smaller pores are only accessible after outgassing at 275 °C. By replacing a fraction of silicon in the imogolite synthesis with germanium, the tube diameter is increased and adsorption properties varied. Despite the narrow pore size distributions expected from the imogolite structure and the microscopy, analysis of the adsorption data using both the Saito–Foley modification of the HK method and the MP/*t*-plot method indicated a much broader pore size distribution (although the mean pore size is reasonable). We attribute this to be due to shortcomings in the adsorption analysis theories rather than that the samples exhibit an actual pore size distribution.

Acknowledgment. This work was supported in part by the UNM/NSF Center for Micro-Engineered Ceramics which is funded by NSF (CDR-8803512), Sandia and Los Alamos National Laboratories, the New Mexico Research and Development Institute, and the Ceramics industry. Additional support was provided for J.K.B. and C.J.B. by Sandia National Laboratories, a U.S. Department of Energy facility operated under Contract DE-AC-04-76DP00789. The TEM work was performed in the Electron Microbeam Analysis Facility in the Department of Geology and Institute of Meteoritics at the University of New Mexico. The authors thank Professor K. Wada of Kyushu University for graciously providing the sample of purified natural imogolite and W. Fahrenholtz and J. Anderson of CMEC for the XRD and SEM work.